

Rare earth doped Si-rich ZnO for multiband near-infrared light emitting devices

Emanuele Francesco Pecora, Thomas I. Murphy, and Luca Dal Negro

Citation: *Appl. Phys. Lett.* **101**, 191115 (2012); doi: 10.1063/1.4766947

View online: <http://dx.doi.org/10.1063/1.4766947>

View Table of Contents: <http://apl.aip.org/resource/1/APPLAB/v101/i19>

Published by the [American Institute of Physics](http://www.aip.org).

Related Articles

The role of cesium carbonate on the electron injection and transport enhancement in organic layer by admittance spectroscopy

Appl. Phys. Lett. **101**, 193303 (2012)

The role of cesium carbonate on the electron injection and transport enhancement in organic layer by admittance spectroscopy

APL: Org. Electron. Photonics **5**, 243 (2012)

Growth and characterization of n-type electron-induced ferromagnetic semiconductor (In,Fe)As

Appl. Phys. Lett. **101**, 182403 (2012)

Probing interfacial charge accumulation in ITO/ α -NPD/Alq3/Al diodes under two electroluminescence operational modes by electric-field induced optical second-harmonic generation

J. Appl. Phys. **112**, 083723 (2012)

Causes of driving voltage rise in phosphorescent organic light emitting devices during prolonged electrical driving

Appl. Phys. Lett. **101**, 173502 (2012)

Additional information on *Appl. Phys. Lett.*

Journal Homepage: <http://apl.aip.org/>

Journal Information: http://apl.aip.org/about/about_the_journal

Top downloads: http://apl.aip.org/features/most_downloaded

Information for Authors: <http://apl.aip.org/authors>

ADVERTISEMENT



Goodfellow
metals • ceramics • polymers • composites
70,000 products
450 different materials
small quantities fast

www.goodfellowusa.com

Rare earth doped Si-rich ZnO for multiband near-infrared light emitting devices

Emanuele Francesco Pecora,¹ Thomas I. Murphy,¹ and Luca Dal Negro^{1,2,a)}

¹Department of Electrical and Computer Engineering and Photonics Center, Boston University, 8 Saint Mary's Street, Boston, Massachusetts 02215, USA

²Division of Materials Science & Engineering, Boston University, 15 Saint Mary's Street, Brookline, Massachusetts 02446, USA

(Received 1 September 2012; accepted 26 October 2012; published online 9 November 2012)

We demonstrate a light emitting material platform based on rare-earth doping of Si-rich ZnO thin films by magnetron sputtering, and we investigate the near-infrared emission properties under both optical and electrical injection. Er and Nd radiative transitions were simultaneously activated due to energy transfer via the ZnO direct bandgap and its luminescent defect centers. Moreover, by incorporating Si atoms, we demonstrate Si-mediated enhancement of photoluminescence in Er-doped ZnO and electroluminescence. These results pave the way to novel Si-compatible light emitters that leverage the optically transparent and electrically conductive ZnO matrix for multiband near-IR telecom and bio-compatible applications. © 2012 American Institute of Physics. [<http://dx.doi.org/10.1063/1.4766947>]

Transparent conductive oxides (TCOs) are a broad class of organic and inorganic materials exhibiting both optical transparency and electrical conductivity simultaneously.¹ TCOs are utilized as top-contact passive layers in a number of optoelectronic devices, including flat panel displays and solar cells.^{2–4} Recently, they are also attracting considerable attention as an active platform for a wide range of novel device applications, ranging from high-performance transistors to optical detectors and emitters in the UV spectral range. Among them, zinc oxide (ZnO) is the most promising candidate for optoelectronic integration due to its low cost, Si compatibility, and radiation hardness. Moreover, ZnO is a direct bandgap ($E_g = 3.3$ eV) material with a large exciton binding energy (60 meV), featuring a wide spectrum of interesting physical properties such as photoconductivity, thermal stability, and piezoelectricity.^{5,6} In addition, it is a biocompatible material and possibly biodegradable.^{7,8} Finally, ZnO has a high refractive index ($n = 2.00$), which could enable novel optically guiding and resonant photonic structures with significant mode confinement⁹ for optoelectronic device integration on a conductive platform in the UV spectral range.^{10–12} Moreover, the optical emission properties of rare earth (RE) atoms in ZnO have been recently investigated for the visible and near-IR spectral range.^{13–16}

In relation to Si-based photonics, Er and Nd ions have been primarily investigated in Si-based dielectric host matrices, such as Si dioxide and Si nitride, for the engineering of efficient near-IR emitters under optical and electrical pumping.^{17–21} Energy sensitization through crystalline or amorphous Si nanoclusters has been recently demonstrated in Er and Nd-doped Si-rich dielectrics leading to significantly enhanced light emission.^{22–24} However, the insulating nature of conventional dielectric host matrices, such as Si dioxide and Si nitride, hampers the development of Si-based emitters under electrical pumping.

In this paper, we propose and demonstrate a novel approach based on the RE-doping of Si-rich ZnO conductive thin films for multiband near-IR light emitting devices under optical and electrical pumping. Er and Nd transitions are observed at 920 nm, 980 nm, 1040 nm, 1350 nm, and 1540 nm under optical pumping, and their excitation mechanism unveiled. Moreover, efficient energy sensitization of Er ions in Si-rich ZnO has been demonstrated along with Er electroluminescence (EL) at low injection current density (40 mA/cm²) in a proof-of-concept device structure.

Er and Nd (co-)doped Si-rich ZnO thin films have been grown on silicon and quartz substrates by magnetron co-sputtering in a Denton Discovery 18 confocal-target system. The base pressure was about 4×10^{-7} mbar, using Ar as a carrier gas. Samples have been grown at room temperature. The film thickness has been fixed at 200 nm. Post annealing processes were performed in a rapid thermal annealing furnace at 900 °C for 200 s in oxygen atmosphere. The elemental composition of the grown materials has been determined with an energy dispersive x-ray spectrometer (Oxford ISIS mounted in a Zeiss Supra 55 Scanning Electron Microscope). The RE content in the samples has been varied by changing the sputtering cathode power, resulting in a Er concentration varying in the range 3.5×10^{19} cm⁻³– 3.0×10^{20} cm⁻³, and Nd concentration in the range 1.2×10^{19} cm⁻³– 3.5×10^{20} cm⁻³. Moreover, RE-doped Si-rich ZnO samples have been fabricated with Si content in the range 2.7×10^{19} cm⁻³– 3.1×10^{20} cm⁻³. Transmission measurements of films deposited on quartz substrates were performed between 200 nm and 1600 nm using a UV/VIS/NIR double beam spectrophotometer (Varian/Agilent Cary 5000). Additionally, the samples were analyzed using variable-angle spectroscopic ellipsometry (J. A. Woollam Co.). Room-temperature photoluminescence (PL) experiments have been performed using a mode-locked high-power ultrafast (150 fs) Ti:sapphire laser (MaiTai HP SpectraPhysics, 82 MHz repetition rate) pumping a second harmonic crystal cavity. Photoluminescence excitation spectroscopy (PLE) has been performed using a

^{a)} Author to whom correspondence should be addressed. Electronic mail: dalnagro@bu.edu.

tunable (340 nm–2200 nm) optical parametric oscillator (SpectraPhysics Inspire) pumped by the Ti:sapphire laser. The PL and PLE signal have been collected through a standard telescoping lens arrangement, dispersed into an f/4 monochromator (Cornerstone 260), and detected using a lock-in amplifier (Oriel Merlin) coupled to a visible-sensitive (Oriel Instrumentation 77348) or an IR-sensitive (Hamamatsu R5509-73) photomultiplier tube. Emission rise-time and lifetime measurements have been conducted pumping the samples with a continuous wavelength Ar ion laser (SpectraPhysics 177-602) modulated by a mechanical chopper and coupling the detector output to an oscilloscope. Current-voltage characteristics of electroluminescent devices were measured using a Keithley 2400-LV SourceMeter. The EL signal was collected through a 5× microscope objective and detected through an optical fiber coupled to an IR-sensitive Ocean Optics spectrometer.

Representative PL spectra of RE-doped ZnO thin films on quartz substrates are shown in Fig. 1. The excitation wavelength was 350 nm, shorter than the ZnO band-gap. In particular, Fig. 1(a) displays the three characteristic PL lines of the Nd-doped ZnO sample, centered at 920 nm, 1080 nm, and 1350 nm, corresponding to transitions originating from the $^4F_{3/2}$ energy level to the $^4I_{9/2}$, $^4I_{11/2}$, and $^4I_{13/2}$ levels, respectively. Panel (b) shows the emission of the Er-doped ZnO sample, with Er-related emission lines clearly distinguishable (the $^4I_{13/2}$ and $^4I_{11/2}$ - $^4I_{15/2}$ transition corresponding to 1540 and 980 nm, respectively). Moreover, multiband emission is clearly observed in Fig. 1(c), which shows the emission of the co-doped sample and demonstrates the ability to co-activate multiple RE in the same ZnO matrix.

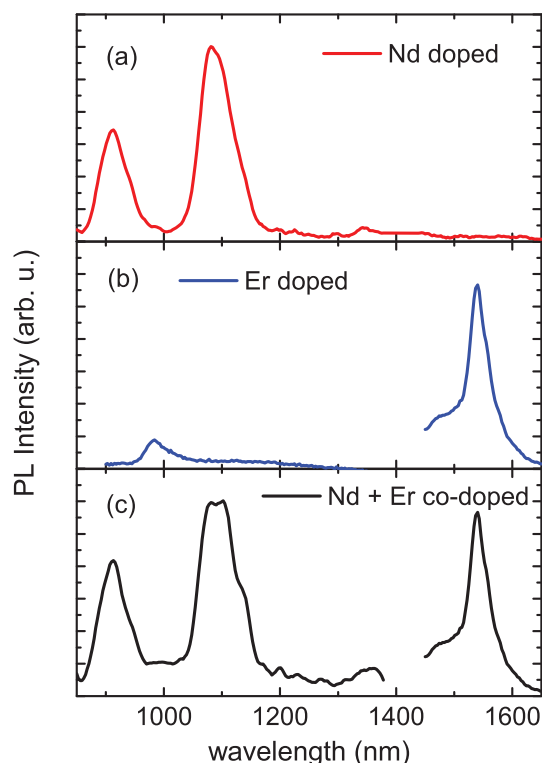


FIG. 1. PL spectra of Er-doped (a), Nd-doped, (b) and Er and Nd co-doped ZnO thin film at an excitation wavelength of 350 nm.

In order to understand the RE excitation mechanisms in ZnO, we have investigated in more detail the optical properties of the fabricated samples. Figure 2(a) shows the transmission spectrum of the reference (i.e., un-doped) ZnO, which features high optical transparency (larger than 80%) extending from the energy band-gap down to the IR. Similar transparency is achieved in the doped materials after the thermal treatment. In the inset, we report the absorption coefficient for the reference and RE-doped ZnO in a Tauc plot, from which we estimate the material optical band-gap by fitting the linear regime of the curves.^{24,25} The optical band gaps are calculated from the Tauc's plot using the relation $\alpha h\nu = \text{const} \times (h\nu - E_{\text{Tauc}})^{1/2}$. The absorption coefficients $\alpha(\lambda)$ of the samples are estimated from the transmission and ellipsometric data, according to the procedure detailed in Ref. 26. We determine a value for the energy gap of 3.23 eV in the ZnO reference sample. On the other hand, the incorporation of RE dopants widens the band-gap up to 3.34 eV for the sample with Nd content of $6.7 \times 10^{19} \text{ cm}^{-3}$. Identical trends are observed for both Er and Nd dopants. It is known in literature that an increase of O-related vacancies in the matrix widens the ZnO band-gap.²⁷ The effect observed in the RE-doped ZnO is also attributed to an increase of the O-vacancies in the matrix, since RE preferentially bond to oxygen atoms,^{28,29} thus increasing the concentration of O-vacancies in the matrix. More interestingly, the incorporation of RE dopants changes dramatically the optical emission properties of the ZnO. In fact, we show in Fig. 2(b) the PL spectra (logarithmic scale) of reference and RE-doped ZnO

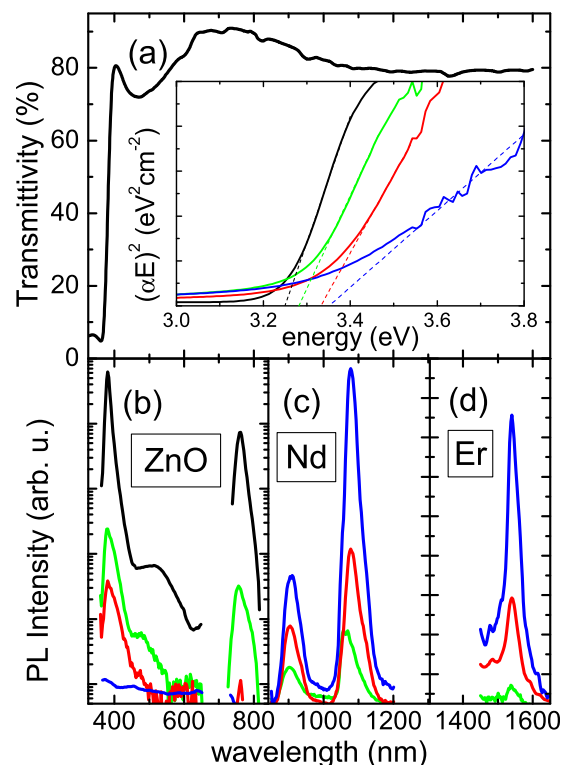


FIG. 2. (a) Transmission spectrum of reference (un-doped) ZnO thin film. (Inset) Tauc plot of the reference and RE-doped ZnO samples. (b) Visible and (c) and (d) near-IR PL spectra of the reference (black line) and RE-doped ZnO thin films at an excitation wavelength of 350 nm. Nd concentration is between $1.2 \times 10^{19} \text{ cm}^{-3}$ (green line) and $6.7 \times 10^{19} \text{ cm}^{-3}$ (blue line); Er concentration is between $3.5 \times 10^{19} \text{ cm}^{-3}$ (green line) and $1.8 \times 10^{20} \text{ cm}^{-3}$ (blue line).

samples pumped at 350 nm. The black line refers to the reference sample. The ZnO direct gap emission occurs around at 385 nm. However, two broader emission bands, centered at 520 and 750 nm, are also observed and are attributed to structural defects, such as oxygen and zinc vacancies or interstitials.³⁰ In addition, we notice that the visible light intensity from the ZnO decreases, and eventually disappears completely, as the RE concentration is increased. On the other hand, under these conditions, we observed a significant increase of the IR light emission from Nd (panel (b)) and Er (panel (c)) ions. The anti-correlation behavior between ZnO-related emission bands and the RE emission indicates that the excitation energy is transferred from the ZnO emitting states (i.e., direct gap and defect bands) to RE centers.

In order to enhance the efficiency of this energy transfer process under optical and electrical pumping, we have fabricated RE-doped Si-rich ZnO thin films. We report in Fig. 3(a) the PL enhancement of the Er and Nd emission, with respect to RE-doped ZnO sample without Si, as a function of the Si content. We notice that the presence of Si is strongly beneficial to the measured Er emission in ZnO, which is enhanced up to one order of magnitude (for the sample with a Si concentration of $1.4 \times 10^{20} \text{ cm}^{-3}$). Moreover, we show in Fig. 3(b) the measured Er emission lifetime values for the samples with varying Si content. We notice that the Er lifetime in the sample without Si is 1.8 ms, which is a significantly long decay time for the ZnO matrix at room

temperature.^{13,14} Moreover, we found that the lifetime of Er decreases as the Si content is increased, and it drops to $500 \mu\text{s}$ in the sample with the highest Si content. We believe that the incorporation of Si additionally introduces a manifold of structural defects in the matrix, which act as non-radiative centers for the optically excited Er ions.^{24,31} This affects the overall photoluminescence efficiency, which in fact decreases at the highest Si concentration, requiring engineering trade-offs between emission sensitization and non-radiative de-excitation. On the other hand, we discovered that increasing the Si concentration in the matrix is always detrimental for the Nd emission, as shown in Fig. 3(a). To better understand the role of Si atoms in the RE emission, we performed PLE spectroscopy for both Er (detection wavelength fixed at 1540 nm) and Nd-doped (detected at 1080 nm) ZnO samples, as shown in Figs. 3(c) and 3(d), respectively. The PLE data are shown in logarithmic scale. In both cases, red circles refer to the samples without Si, and blue squares to Si-rich samples. We notice that, in the case of the samples without Si, Er and Nd ions can be excited either on resonance with their electronic transitions (labeled in the panel) or via the photo-generated carriers above the ZnO gap at wavelengths shorter than 390 nm. On the other hand, the incorporation of Si in Er-doped ZnO substantially broadens the Er excitation spectrum demonstrating off-resonance Er excitation due to energy-transfer. Contrarily, we do not observe off-resonance excitation in Nd-doped Si-rich

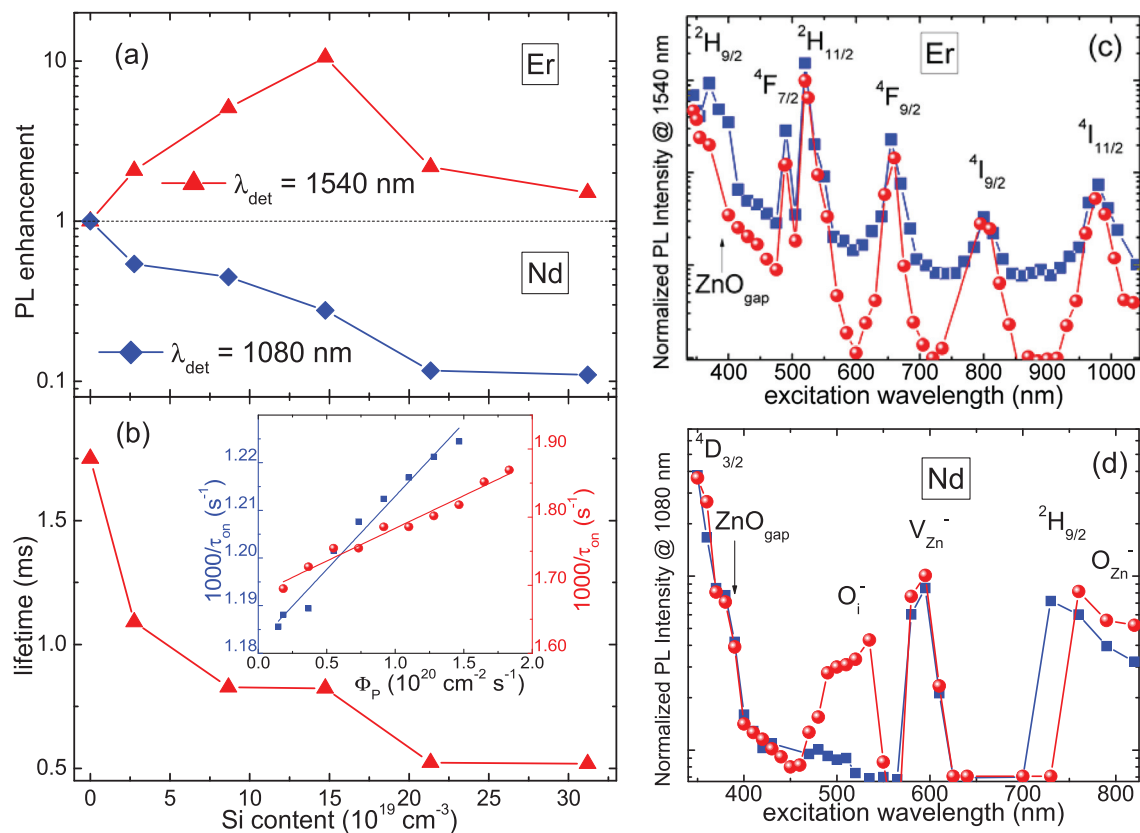


FIG. 3. (a) PL enhancement of the Er and Nd emissions as a function of the Si content in the ZnO samples. The excitation wavelength was 350 nm. (b) Measured Er emission lifetime as a function of the Si content. Pump power was 20 mW. (Inset) Inverse of the Er emission risetime as a function of the pumping photon flux (Φ_p) measured in Er-doped ZnO sample without Si (red circles, right hand scale) and Si-rich (blue squares, left hand scale). Si content was $1.4 \times 10^{20} \text{ cm}^{-3}$; Er content was $1.8 \times 10^{20} \text{ cm}^{-3}$. Emission risetime and lifetime traces were measured at the excitation wavelength of 488 nm. (c) PLE spectroscopy for Er-doped (detection wavelength: 1540 nm) and (d) Nd-doped (detection wavelength: 1080 nm) ZnO thin films with and without Si. Red circles refer to the samples without Si and blue squares to the Si-rich samples. All the PLE spectra have been normalized to their values at 350 nm to facilitate comparison.

samples, due to the absence of Nd-related (acceptor) transitions overlapping with the manifold of Si-related donor centers in the matrix.³² However, the non-radiative energy channels introduced with the Si excess reduce the Nd PL efficiency, as shown in Fig. 3(a). In general, we expect that the Nd emission can be sensitized by the luminescent centers associated to interstitial oxygen (O_i) and zinc vacancies (V_{Zn}).³⁰ However, in the Si-rich Nd-doped sample, we do not detect any Nd PL sensitization when pumping at around 500 nm. This is consistent with the formation of Si-O bonds that quenches the density of O_i , inhibiting the transfer of energy to the Nd ions.

In order to quantify the matrix-mediated energy transfer to Er ions, we have measured the effective excitation cross section of Er from the linear dependence of the Er PL rise-time versus the pumping photon flux,^{23,24,33} as shown in the inset of Fig. 3(b). The experimentally measured cross section for the Si-rich sample is $1.9 \times 10^{-18} \text{ cm}^{-2}$, while for Er-doped ZnO without Si is $7.6 \times 10^{-20} \text{ cm}^{-2}$. The Er decay time extracted from the intercept in the plot is approximately 1.9 ms for the sample without Si and 846 μs for the Si-rich ZnO sample, in agreement with the directly measured Er lifetime values. The data shown in the inset of Fig. 3(b) clearly demonstrate energy transfer to Er via Si-related donor centers in ZnO with almost 25 times enhanced excitation cross section.

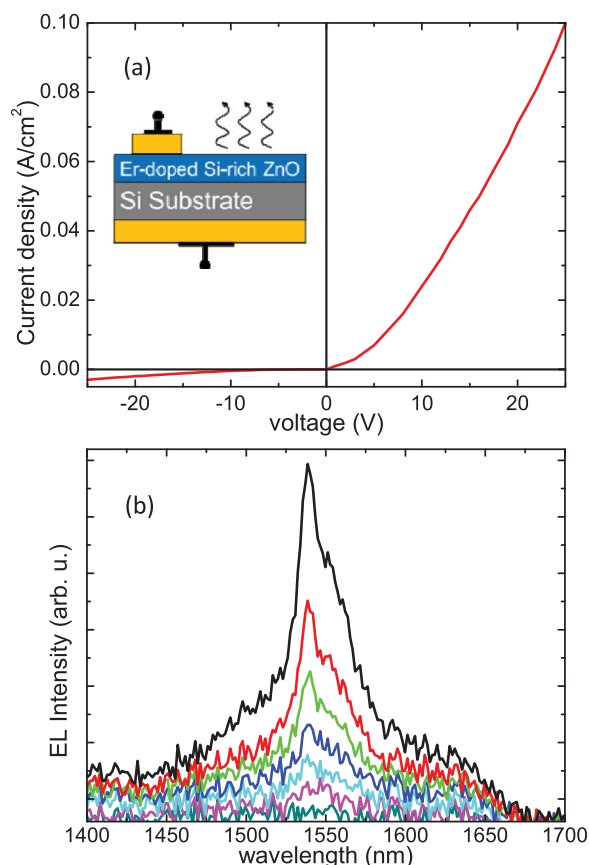


FIG. 4. (a) Current density versus the applied voltage measured in a proof-of-concept electroluminescent device with Er-doped Si-rich ZnO active layer ($1.4 \times 10^{20} \text{ Si/cm}^{-3}$; $1.8 \times 10^{20} \text{ Er/cm}^{-3}$). (Inset) Schematic picture of the device. (b) EL spectra collected from the Er-doped Si-rich ZnO electroluminescent device at different current densities in the range between 40 mA/cm^2 (teal line) and 80 mA/cm^2 (black line) with 6.6 mA/cm^2 steps.

Finally, we demonstrate the potential of the Er-doped Si-rich ZnO platform by fabricating a proof-of-concept electroluminescent device. The device structure is shown in the inset of Fig. 4(a). We used the optimized material (with a Si content of $1.4 \times 10^{20} \text{ cm}^{-3}$ and Er content of $1.8 \times 10^{20} \text{ Er/cm}^3$) as active layer on a p^+ -type Si substrate, and we evaporated a thin (60 nm) Au layer as back-contact and as a front pad. The current density plotted as a function of the applied voltage is shown in Fig. 4(a). The device shows a rectifying behavior with low turn-on voltage (1.5 V). In Fig. 4(b), we show the EL spectra collected at different current densities in the range between 40 mA/cm^2 and 80 mA/cm^2 . It should be noted that the injected current densities are low compared to the state-of-the-art in Si-based light emitters.^{34,35}

In conclusion, we have demonstrated that ZnO can be effectively utilized as an active layer for RE light emission in the IR on a Si platform. We have investigated the RE excitation mechanism, which is driven by energy transfer from the ZnO band-gap under optical emission. Moreover, we introduce Si in the matrix and demonstrate efficient Si-mediated energy sensitization of Er emission. Furthermore, we demonstrate electroluminescence in Er-doped Si-rich ZnO under low injection current density. These findings pave the way for a novel Si-compatible material platform for on-chip bio-compatible IR light emitting devices.

This work was partly supported by the AFOSR program “Deterministic Aperiodic Structures for On-chip Nanophotonic and Nanoplasmonic Device Applications,” under Award FA9550-10-1-0019, and by the NSF Career Award No. ECCS-0846651. T.M. acknowledges the National Science Foundation (Award NSFEEC-1009808) for the financial support.

¹J. F. Wager, *Science* **300**, 1245 (2003).

²T. Minami, S. Takata, and T. Kakumu, *J. Vac. Sci. Technol. A* **14**, 1689 (1996).

³H. Kawazoe, M. Yasukawa, H. Hyodo, M. Kurita, H. Yanagi, and H. Hosono, *Nature* **389**, 939 (1997).

⁴E. Fortunato, D. Ginley, H. Hosono, and D. C. Paine, *MRS Bull.* **32**, 242 (2007).

⁵Z. Fan, D. Dutta, C. Chien, H. Chen, E. Brown, P. Chang, and J. Lu, *Appl. Phys. Lett.* **89**, 213110 (2006).

⁶Z. L. Wang and J. Song, *Science* **312**, 242 (2006).

⁷J. Zhou, N. S. Xu, and Z. L. Wang, *Adv. Mater.* **18**, 2432 (2006).

⁸Z. Li, R. Yang, M. Yu, F. Bai, C. Li, and Z. L. Wang, *J. Phys. Chem. C* **112**, 20114 (2008).

⁹M. Wu, A. Azuma, T. Shiosaki, and A. Kawabata, *J. Appl. Phys.* **62**, 2482 (1987).

¹⁰M. H. Huang, S. Mao, H. Feick, H. Yan, Y. Wu, H. Kind, E. Weber, R. Russo, and P. D. Yang, *Science* **292**, 1897 (2001).

¹¹P. Yang, H. Yan, S. Mao, R. Russo, J. Johnson, R. Saykally, N. Morris, J. Pham, R. He, and H. Choi, *Adv. Funct. Mater.* **12**, 323 (2002).

¹²J. Lim, C. Kang, K. Kim, I. Park, D. Hwang, and S. Park, *Adv. Mater.* **18**, 2720 (2006).

¹³S. Komuro, T. Katsumata, T. Morikawa, X. Zhao, H. Isshiki, and Y. Aoyagi, *Appl. Phys. Lett.* **76**, 3935 (2000).

¹⁴S. Komuro, T. Katsumata, T. Morikawa, X. Zhao, H. Isshiki, and Y. Aoyagi, *J. Appl. Phys.* **88**, 7129 (2000).

¹⁵Y. R. Jang, K. H. Yoo, J. S. Ahn, C. Kim, and S. M. Park, *Appl. Surf. Sci.* **257**, 2822 (2011).

¹⁶D. Wang, G. Xing, M. Gao, L. Yang, J. Yang, and T. Wu, *J. Phys. Chem. C* **115**, 22729 (2011).

¹⁷G. Franzò, V. Vinciguerra, and F. Priolo, *Appl. Phys. A* **69**, 3 (1999).

¹⁸N. Daldosso, D. Navarro-Urrios, M. Melchiorri, L. Pavesi, F. Gourbilleau, M. Carrada, R. Rizk, C. Garcia, P. Pellegrino, B. Garrido, and L. Cognolato, *Appl. Phys. Lett.* **86**, 261103 (2005).

- ¹⁹D. Breard, F. Gourbilleau, C. Dufour, R. Rizk, J. Doualan, and P. Camy, *Mater. Sci. Eng. B* **146**, 179 (2008).
- ²⁰R. Li, S. Yerci, S. O. Kucheyev, T. van Buuren, and L. Dal Negro, *Opt. Express* **19**, 5379 (2011).
- ²¹R. Li, S. Yerci, and L. Dal Negro, *Appl. Phys. Lett.* **95**, 041111 (2009).
- ²²M. Fujii, M. Yoshida, Y. Kanzawa, S. Hayashi, and K. Yamamoto, *Appl. Phys. Lett.* **71**, 1198 (1997).
- ²³F. Priolo, G. Franzò, D. Pacifici, V. Vinciguerra, F. Iacona, and A. Irrera, *J. Appl. Phys.* **89**, 264 (2001).
- ²⁴S. Yerci, R. Li, S. O. Kucheyev, T. van Buuren, S. N. Basu, and L. Dal Negro, *Appl. Phys. Lett.* **95**, 031107 (2009).
- ²⁵C. Gumus, O. M. Ozkendir, H. Kavak, and Y. Ufuktepe, *J. Opt. Adv. Mater.* **8**, 299 (2006). Available at: http://joam.inoe.ro/arhiva/pdf8_1/Gumus1.pdf.
- ²⁶S. Yerci, R. Li, O. Kucheyev, T. van Buuren, S. N. Basu, and L. Dal Negro, *IEEE J. Sel Top. Quantum Electr.* **16**, 114 (2010).
- ²⁷Y. Chen and X. L. Xu, *Phys. B* **406**, 3121 (2011).
- ²⁸P. N. Favennec, H. Haridon, D. Moutonnet, M. Salvi, and M. Gauneau, *Jpn. J. Appl. Phys.* **29**, L524 (1990).
- ²⁹A. Polman, *Phys. B* **300**, 78 (2001).
- ³⁰B. Lin, Z. Fu, and Y. Jia, *Appl. Phys. Lett.* **79**, 943 (2001).
- ³¹G. Franzò, E. Pecora, F. Priolo, and F. Iacona, *Appl. Phys. Lett.* **90**, 183102 (2007).
- ³²L. Lai, C. Liu, C. Lee, L. Lou, W. Yeh, and M. Chu, *J. Mater. Res.* **23**, 2506 (2008).
- ³³D. Pacifici, G. Franzò, F. Priolo, F. Iacona, and L. Dal Negro, *Phys. Rev. B* **67**, 245301 (2003).
- ³⁴S. Yerci, R. Li, and L. Dal Negro, *Appl. Phys. Lett.* **97**, 081109 (2010).
- ³⁵S. Iwan, S. Bambang, J. L. Zhao, S. T. Tan, H. M. Fan, L. Sun, S. Zhang, H. H. Ryu, and X. W. Sun, *Phys. B* **407**, 2721 (2012).